Stellar Rotation
Proceedings IAU Symposium No. 215, © *2003 IAU*
André Maeder & Philippe Eenens, eds.

Presupernova Evolution of Rotating Massive Stars and the Rotation Rate of Pulsars

A. Heger

Department of Astronomy and Astrophysics, Enrico Fermi Institute, University of Chicago, 5640 S. Ellis Avenue, Chicago IL 60637, USA

S. E. Woosley

Department of Astronomy and Astrophysics, UCSC, Santa Cruz CA 95064, USA

N. Langer

Astronomical Institute, P.O. Box 80000, NL-3508 TA Utrecht, The Netherlands

H. C. Spruit

Max-Plank-Institut für Astrophysik, Karl-Schwarzschild Str. 1, 85740 Garching, Germany

Abstract. Rotation in massive stars has been studied on the main sequence and during helium burning for decades, but only recently have realistic numerical simulations followed the transport of angular momentum that occurs during more advanced stages of evolution. The results affect such interesting issues as whether rotation is important to the explosion mechanism, whether supernovae are strong sources of gravitational radiation, the star's nucleosynthesis, and the initial rotation rate of neutron stars and black holes. We find that when only hydrodynamic instabilities (shear, Eddington-Sweet, etc.) are included in the calculation, one obtains neutron stars spinning at close to critical rotation at their surface – or even formally in excess of critical. When recent estimates of magnetic torques (Spruit 2002) are added, however, the evolved cores spin about an order of magnitude slower. This is still more angular momentum than observed in young pulsars, but too slow for the collapsar model for gamma-ray bursts.

1. Introduction

Stars more massive than about $8 - 10\,\mathrm{M}_\odot$ end their life as supernova, leaving a compact remnant - a neutron star or a black hole. Generally speaking, the evolution of such a star follows a well understood path of contraction to increasing central density and temperature. This path of contraction is interrupted by nuclear fusion – first hydrogen to helium, then helium to carbon and oxygen, followed by carbon, neon, oxygen, and silicon burning, until finally a core of iron is produced. Each fuel burns first in the center of the star, then in one or more shells. In Table 1 we summarize the burning stages and their durations for a $20\,M_\odot$ star. The time scale for helium burning is about ten times shorter than that of hydrogen burning, mostly because of the lower energy release per unit mass. The time scale of the burning stages and contraction beyond central helium-burning is greatly reduced by thermal neutrino losses that carry away energy *in situ*, instead of requiring that it be transported to the stellar surface by diffusion or convection. These losses increase with temperature as roughly T^9 (see Woosley, Heger & Weaver for a more extended review). When the star has built up a large enough iron core, exceeding its effective Chandrasekhar mass, it collapses to form a neutron star or a black hole. A supernova explosion may result (e.g., Colgate & White 1966), or, in rare cases, a gamma-ray burst (Woosley 1993; MacFadyen & Woosley 1999; MacFadyen, Woosley, & Heger 2001).

Unevolved massive stars, however, are known to rotate rapidly at several times 10 % of their break-up velocity at the surface. Characteristic values of the equatorial rotation velocity on the main sequence are around $\sim 200\,\mathrm{km\,s^{-1}}$ (Fukuda 1982; and other contributions in these proceedings). In this paper, we address what happens to the rotation in the interior of these stars as they evolve. In general, the ongoing contraction leads to faster rotation, but transport processes (circulation, viscosity, magnetic fields, etc.) lead to loss of angular momentum from the stellar core. We are particularly interested in the model predictions for the rotational periods of the collapsed remnants left by the supernova.

2. Rotating stars

2.1. Angular momentum transport

On the main sequence, massive stars quickly settle into rigid rotation (e.g., Zahn 1992; Talon et al. 1997, Meynet & Maeder 2000; Maeder & Meynet 2000). Contraction increases the rotational energy faster than gravitational binding energy and would eventually make the core unstable to triaxial deformations (Ostriker & Bodenheimer 1973). Without the transport of angular momentum, for typi-

Table 1. Nuclear burning stages in massive stars. The table gives burning stages, main products (ashes), typical temperatures, and time scales for a $20\,M_\odot$ star.

Fuel	Main Product	T (10^9 K)	duration (yr)
H	He	0.037	8.1×10^6
He	O, C	0.19	1.2×10^6
C	Ne, Mg	0.87	9.8×10^2
Ne	O, Mg	1.6	0.60
O	Si, S	2.0	1.3
Si	Fe	3.3	0.031

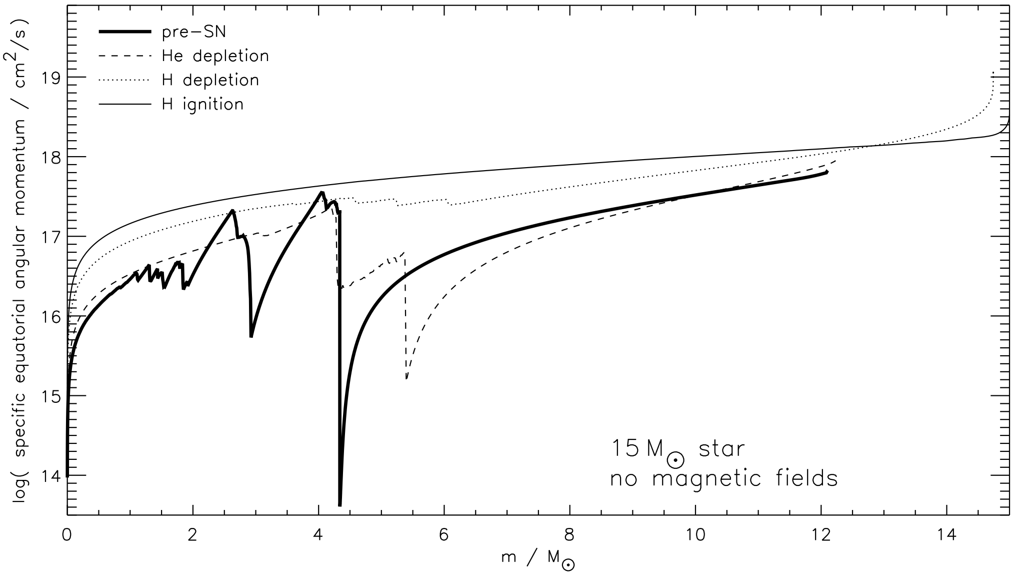

Figure 1. Specific angular momentum, j, as a function of mass coordinate, m at different evolution stages in $15\,\mathrm{M}_\odot$ star rotating with $200\,\mathrm{km\,s^{-1}}$ on the zero-age main sequence (ZAMS; hydrogen ignition). The *thin sold line* gives j on the ZAMS at which the star is essentially in rigid rotation. The *dotted line* gives the angular momentum at central hydrogen depletion (1 % hydrogen left), the *dashed line* at central helium depletion (1 % helium left), and the *thick solid line* the distribution at onset of core collapse. The lines of later evolution stages end at lower mass coordinate because of mass loss due to stellar winds.

cal initial rotation rates, this would happen during central helium burning, but clearly the transport of angular momentum in the stellar interior cannot be neglected. Important processes for angular momentum transport include hydrodynamic instabilities (convection, shear, circulation, etc.; see, e.g., Endal & Sofia 1978; Knobloch & Spruit 1983; Heger, Langer, Woosley 2000; Tassoul 2000) and magnetic fields (e.g., Spruit & Phinney 1998; Spruit 2002). The instabilities, however, are inhibited by thermal, and, most importantly, compositional stratification inside the star (e.g., Kippenhahn 1974, Knobloch & Spruit 1983; Maeder & Meynet 1997; Maeder 2003).

Early calculations by Kippenhahn & Thomas (1970); Kippenhahn, Meyer-Hofmeister, & Thomas (1970) and by Endal & Sofia (1976) that ignored angular momentum transport, or only included it in chemically homogeneous regions, did indeed find that the star became secularly unstable at the end of central helium burning or reached critical rotation before central carbon burning. Later models by Endal & Sofia (1978), that considered Eddington-Sweet circulation (Eddington 1924, 1929; Vogt 1925), shear instabilities (e.g., Zahn 1974, 1975; Maeder 1997), GSF instability (Goldreich & Schubert 1967; Fricke 1968), and Solberg-Høiland instability (Wasiutyński 1946) found significant transport of angular momentum that allowed their stars to go well beyond central carbon burning without reaching the limit of secular instability. Still the models rotated about three times faster, after central helium burning, than the more recent models of Heger, Langer & Woosley (2000). This more recent study reduced the efficiency of composition gradients in inhibiting instabilities and of compositional mixing relative to angular momentum transport (Pinsonneault et al. 1989; Chaboyer & Zahn 1992) in order to reproduce observed stellar surface abundance anomalies (e.g., Giess & Lambert 1992; Venn et al. 2002). Calculations by the Geneva Group also found, after central helium burning, rotation rates similar to those of Heger et al. (2000; Maeder, private communication) and the most recent calculations by Hirschi, Meynet, & Maeder (2003) find comparable rotation rates during oxygen shell burning, $0.16\,\mathrm{rad\,s^{-1}}$ in $15\,\mathrm{M_\odot}$ star of initially $300\,\mathrm{km\,s^{-1}}$ compared to $0.12\,\mathrm{rad\,s^{-1}}$ for a star with initially $200\,\mathrm{km\,s^{-1}}$ in Heger et al. Others have also studied massive star rotation, but concentrated on the main sequence and helium burning (e.g., Urpin, Shalybkov, & Spruit 1996; Talon & Zahn 1997; Denissenkov, Ivanova, & Weiss 1999).

2.2. Mixing

Rotation also causes mixing even in regions that, without rotation, are stably stratified. For a review of mixing processes in stars, see Pinsonneault (1997). Observational evidence for this is the surface enrichment of elements produced deep inside the star. For example, an enrichment of nitrogen with respect to oxygen and carbon, or of helium, and the depletion of boron during central hydrogen burning (e.g., Giess & Lambert 1992; Venn et al. 2002; Fliegner, Langer, & Venn 1996). The enrichment of helium above the convective core during central hydrogen burning can also lead to an increase of the luminosity similar to core overshooting that was often assumed in non-rotating stellar models.

During central helium burning, rotationally-induced mixing can prevent the formation of layering in the convective core (Heger et al. 2002). If the mixing

Table 2. Evolution of the internal stellar rotation for a $15\,\mathrm{M_\odot}$ star. The first column gives the evolution stage (see explanation below), the second column gives the central density at this evolution stage, the 3^{rd} column gives the specific angular momentum at a mass coordinate of $1.7\,\mathrm{M_\odot}$, and the last three columns give the radius, the angular velocity, and it's ratio to local Keplerian angular velocity at this point. For the neutron star (NS) we have put the values in excess of critical rotation in brackets.

Evolution stage	ρ_c $(\mathrm{g\,cm^3})$	j $(\mathrm{cm^2\,s^{-1}})$	r (cm)	ω $(\mathrm{rad\,s^{-1}})$	$\omega/\omega_\mathrm{Kepler}$
ZAMS[a]	5.8	1.4×10^{17}	6.2×10^{10}	5.6×10^{-5}	0.058
TAMS[b]	11.7	8.9×10^{16}	4.6×10^{10}	6.3×10^{-4}	0.041
He depletion[c]	2800	3.7×10^{16}	8.0×10^{9}	8.6×10^{-4}	0.041
pre-SN[d]	6×10^{9}	2.8×10^{16}	2.8×10^{8}	0.56	0.17
neutron star[e]	4×10^{14}	(2.5×10^{16})	1.2×10^{6}	(3.4×10^{4})	(3)

[a] 2 % hydrogen burnt;
[b] 1 % hydrogen left in the core;
[c] 1 % helium left in the core;
[d] core collapse velocity reaches $1000\,\mathrm{km\,s^{-1}}$;
[e] for a $1.7\,\mathrm{M_\odot}$ core collapsing to a neutron star with moment of inertia $I = 1.44\times10^{45}\,\mathrm{g\,cm^2}$ and assuming no angular momentum loss.

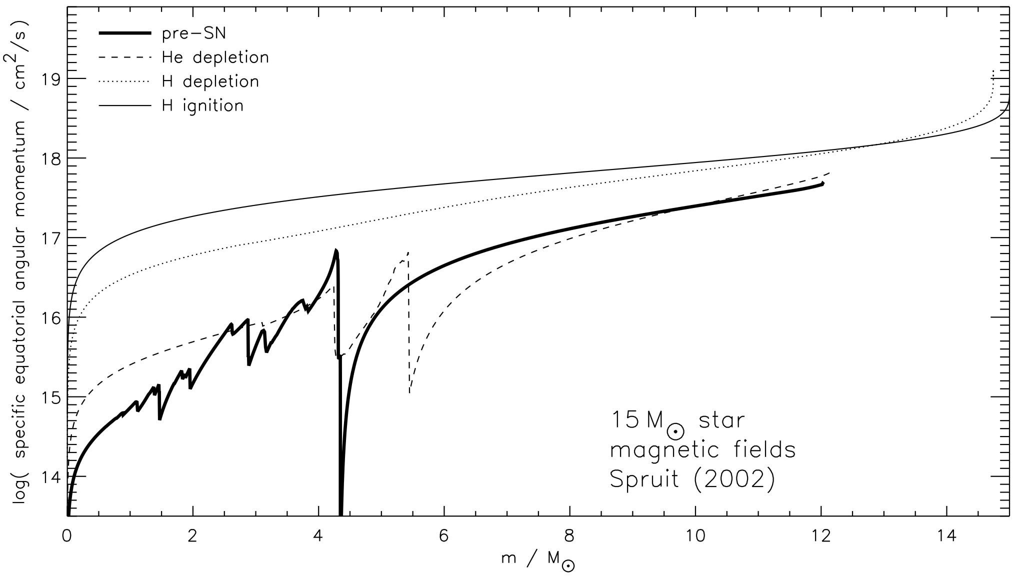

Figure 2. Similar to Figure 1, but for a star that includes magnetic torques according to Spruit (2002, 2003).

above the convective core is fast enough, carbon and oxygen can even be mixed outwards into hydrogen-rich regions and make primary nitrogen, though more typically in stars of solar metallicity, this is suppressed by a rise in entropy and the composition barrier at the base of the hydrogen shell. Additionally, the ratio of circulation time-scale to evolutionary time is smaller than during hydrogen burning, unless the core is spinning faster ($\tau_{\rm circ} \propto \tau_{\rm KH}(\Omega/\Omega_{\rm crit})^2$). Note in particular, that hydrogen cannot be mixed down into the core, since it will rapidly burn at the higher temperatures further down in the star. However, for stars of very low or zero metallicity, this barrier is reduced and some primary nitrogen is made (e.g., Heger, Woosley, & Waters 2000a; Meynet & Maeder 2002; Marigo, Chiosi, & Kudritzki 2003). Unfortunately, the "mixing events" in such stars are currently not well modeled and the amount of primary N^{14} produced is not predicted very reliably.

Since the energy loss to neutrinos accelerates the later burning stages, most rotationally-induced instabilities become too slow to mix radiative regions

Table 3. Experimental periods (Marshall et al. 1998) and angular momentum estimates for young pulsars.

pulsar	period (ms)	j ($\mathrm{cm^2\,s^{-1}}$)	J (erg s)
PSR J0537-6910 (N157B, LMC)	16	2.0×10^{14}	5.67×10^{47}
PSR B0531+21 (crab)	33	9.9×10^{13}	2.75×10^{47}
PSR B0540-69 (LMC)	50	6.5×10^{13}	1.81×10^{47}
PSR B1509-58	150	2.2×10^{13}	6.05×10^{46}

(Heger et al. 2000), though shear instabilities may still function at convective boundaries (see also Hirschi et al. 2003 in these proceedings).

2.3. Evolution till core collapse and pulsar rotation

In Figure 1 we give the evolution of the internal rotation profile for a $15\,\mathrm{M}_\odot$ star and, in Table 2, numerical values for the specific angular momentum, radius, and angular velocity at a mass coordinate of $m = 1.7\,\mathrm{M}_\odot$. This corresponds to the edge of the neutron star that forms later.

During hydrogen burning, angular momentum loss by stellar winds and the contraction of a core bounded by an expanding envelope leads to angular momentum loss from the core. As a gradient in mean molecular weight develops, however, angular momentum gets "trapped" in the core and differential rotation develops between the core and envelope. By the end of central helium burning, rotation in the core is reduced by another factor of two. This is, in part, because the growing core incorporates material of low angular momentum that had been slowed down during the first dredge-up, and, in part, due to angular momentum transport. After central helium burning, hydrodynamic rotationally-induced instabilities are not fast enough for significant angular momentum transport (see above) and angular momentum is essentially locally trapped in the cores of different composition. Only convection is fast enough to redistribute angular momentum over larger regions of the stars and the rigidly rotating convective

Table 4. Magnetic Field and angular velocity evolution in a $15\,\mathrm{M}_\odot$ star of solar composition and $200\,\mathrm{km\,s^{-1}}$ equatorial surface rotation on the ZAMS. We give typical toroidal (B_r) and radial (B_ϕ) magnetic field strengths in the inner 1-2 $\mathrm{M}_\odot$ if radiative or outside the convective core for different evolution stages (see below), and the central angular velocity.

evolution stage	B_ϕ (G)	B_r (G)	Ω_c ($\mathrm{rad\,s^{-1}}$)
MS[a]	5×10^3	1	5.7×10^{-5}
TAMS[b]	1×10^4	2	2×10^{-5}
He ignition[c] ..	4×10^4	30	8×10^{-5}
He depletion[d]	1×10^4	2	6×10^{-5}
C ignition[e] ...	1×10^6	300	2.5×10^{-4}
C depletion[f] .	3×10^7	5×10^3	2×10^{-3}
O depletion[g] .	5×10^7	7×10^3	4×10^{-3}
Si depletion[h] .	3×10^8	2×10^5	7×10^{-3}
pre-SN[i]	5×10^9	10^6	0.1

[a]20 % hydrogen burnt;
[b]1 % hydrogen left in the core;
[c]1 % helium burnt;
[d]1 % helium left in the core;
[e]central temperature of 5×10^8 K;
[f]central temperature of 1.2×10^9 K;
[g]central oxygen mass fraction drops below 5 %;
[h]central Si mass fraction drops below 10^{-4};
[i]infall velocity reaches $1000\,\mathrm{km\,s^{-1}}$.

shells leave an imprint in the rotation profile that are each characterized by a steep drop of the specific angular momentum at its base since, typically, the inner radius of such a shells is much smaller than its outer radius.

In the case of a $15\,M_\odot$ star (solar metallicity) with an initial rotation rate of $200\,\mathrm{km\,s^{-1}}$ the core spins fast enough to form a neutron star in excess of critical rotation (last line of Table 2) if no further loss of angular momentum occurs. Since rotation close to breakup clearly is in contradiction to the rotation rates of young pulsars (Table 3) some additional spin-down is necessary. However, this much rotation in collapsing massive star cores would be preferable for the "collapsar" model for gamma-ray bursts (Woosley 1993). For some time, the r-mode instability (e.g., Lindblom, Tohline, & Vallisneri 2001) seemed to be a promising explanation for spin-down, so that both slow pulsars and collapsars could result from rapidly rotating core, but recent evaluation (Arras et al. 2003) seem to indicate that it may be not efficient enough (see also Woosley & Heger 2003 in these proceedings). An alternative possibility for removing this discrepancy may be angular momentum transport by magnetic fields.

3. Magnetic stars

Spruit & Phinney (1998) assumed that differential rotation would torque an initially arbitrarily weak radial field component into a toroidal field, that, when strong enough, would become unstable, producing a new radial field that is wound up again. With such strong fields they obtained a star that was kept in rigid rotation until about central carbon burning and estimated pulsar rotation rates at birth $\sim 100\,\mathrm{s}$ result. If mass loss is taken into account, the resulting spin would have been even lower by orders of magnitude.

In a more recent approach, Spruit (2002) introduced a dynamo model that considers stabilization of the stratification by thermal and chemical stratification (see also Spruit 2003 in these proceedings). It is assumed that the dynamo reaches a steady state field on a time-scale short compared to that on which the structure and rotation profile of the star evolve. From this dynamo and its equilibrium field an effective diffusivity for chemical mixing and an effective viscosity for angular momentum transport can be derived (Spruit 2002). We

Table 5. Pulsar rotation and angular momentum for different masses. We assume initial solar composition and a ZAMS equatorial surface rotation rate of $200\,\mathrm{km\,s^{-1}}$. In the 2^{nd} column we give the total angular momentum in the inner $1.7\,M_\odot$ of the stellar core. Assuming no further loss of angular momentum and that a neutron star with moment of inertia $I = 1.44\times10^{45}\,\mathrm{g\,cm^2}$ is formed ($R = 12\,\mathrm{km}$, $M = 1.4\,M_\odot$, $I = 0.36MR^2$; Lattimer & Prakash 2001) the resulting (lower limits for the) pulsar periods are given in the 3^{rd} column.

stellar mass	J (erg s)	period (ms)
$15\,M_\odot$	1.4×10^{48}	6.7
$20\,M_\odot$	1.8×10^{48}	5.0
$25\,M_\odot$	2.1×10^{48}	4.3

have implemented both as time-dependent diffusive processes (Heger, Woosley, & Spruit 2003). The results for a $15\,\mathrm{M}_\odot$ model with the same initial properties as in Figure 1 and Table 2, but now including the dynamo process, is given in Figure 2 and Table 4. At the end of central hydrogen burning the star is essentially still in solid body rotation – the small steps seen in Figure 1 between $4-6\,\mathrm{M}_\odot$, marking the composition gradient left behind by central hydrogen burning, are not present – and it rotates significantly slower. By the end of central helium burning, the core is slowed down even further. At this point it rotates at less than a tenth the speed of the non-magnetic star. From here to core collapse the angular momentum in the inner $2\,\mathrm{M}_\odot$ is reduced by an additional factor ~ 3. Despite significant differential rotation, essentially no angular momentum is transported across the edge of the helium core where entropy strongly increases. In Table 4 we also give the central angular velocity at late evolution stages until core collapse along with the equilibrium radial and toroidal magnetic fields. This compilation demonstrates an important property of of Spruit's model: the radial field component is much weaker than the toroidal field component. This is also one of the significant differences with the model of Spruit & Phinney (1998). From these stellar models we obtain neutron star rotation rates of $\sim 4-7\,\mathrm{ms}$ for $15-25\,\mathrm{M}_\odot$ stars assuming all the angular momentum in the core were conserved to for a neutron star (Table 5) and the remnants of more massive stars are rotating faster. These rotation rates are still faster than that of observed young pulsars (Table 4) and additional spin-down mechanisms are still needed to reduce the discrepancy (see Woosley & Heger 2003 in these proceedings). In the derivation of the dynamo model by Spruit (2002) several quantities of "comparable size" have been set equal, introducing parameters "of the order unity" in the theory. Most significant for the angular momentum transport and the presence of effective barriers, like the edge of the helium core mentioned above, are the influence of stabilization of the stratification by thermal and compositional buoyancy. We have varied both, as well as the overall

Table 6. Pulsar rotation rate dependence on dynamo model parameters. For three different initial stellar masses of stars with solar metallicity and ZAMS equatorial surface rotation rate of $200\,\mathrm{km\,s^{-1}}$ we give in the second column the resulting neutron stars period (in ms) for a neutron star of assumed moment of inertia $I = 1.44\times10^{45}\,\mathrm{g\,cm^2}$ of which we assume if forms form the inner $1.7\,\mathrm{M}_\odot$ of the core of the star without further loss of angular momentum. The 3^{rd} and 4^{th} column give the resulting period when the sensitivity to composition gradients is lowered and raised by a factor 10. The 5^{th} and 6^{th} column give the result for a similar modification of thermal buoyancy, and in the last two columns we give when the over-all magnetic stress ($\sim B_\phi B_r$) is modified by a factor 10 in both directions.

initial mass	"std."	N_μ^2		N_T^2		$B_\phi B_r$	
		0.1	10	0.1	10	0.1	10
	period (ms)						
$15\,\mathrm{M}_\odot$	6.7	15	3.8	8.7	6.0	4.3	15
$20\,\mathrm{M}_\odot$	5.0	11	2.3	5.3	4.4	2.8	9.6
$25\,\mathrm{M}_\odot$	4.3	7.6	2.2	3.9	3.6	2.1	6.9

magnetic stress from the dynamo by a factor 10 up and down (Table 6). Even these large variation only result in variations of the neutron star rotation by about a factor ~ 2. The reason for the smallness of the effect is that the stress resulting from the dynamo scales as the $6^{\rm th}$ power of the shear rate.

4. Summary and conclusions

Without the action of magnetic fields, hydrodynamic rotationally-induced instabilities and convection alone (Figure 1) do not transport angular momentum efficiently enough to avoid forming pulsars rotating at break up (assuming that most of the angular momentum is conserved during the collapse; Table 2). When a dynamo process like that of Spruit (2002) is included in the models (Table 4 and Figure 2), one obtains pulsar periods more than a factor 10 slower, about $4-7$ ms (Table 5). Though these periods may still increase by 20 % due to neutrino losses from the proto-neutron star, they are still too fast compared even to the fastest-rotating observed young pulsars (Table 3) and additional spin-down mechanisms may still be needed in single stars (see Woosley & Heger 2003 in these proceedings). However, the rotation rates found in the magnetic stellar models would be too slow for most current gamma-ray burst models which require rapidly rotating stellar cores. However, interacting close binary stars may lead to much faster or slower core rotation, and, e.g., to pulsars of up to a second spin period (Langer et al. 2003).

This research has been supported by the NSF (AST 02-06111), NASA (NAG5-12036), and the DOE Program for Scientific Discovery through Advanced Computing (SciDAC; DE-FC02-01ER41176). AH is supported, in part, by the Department of Energy under grant B341495 to the Center for Astrophysical Thermonuclear Flashes at the University of Chicago, and a Fermi Fellowship at the University of Chicago.

References

Arras, P., Flanagan, E. E., Morsink, S. M., Schenk, A. K., Teukolsky, S. A., & Wasserman, I. 2003, submitted to ApJ, astro ph-0202345

Chaboyer, B., Zahn, J.-P. 1992, A&A, 253, 173

Colgate, S. A., & White, R. H. 1966, ApJ, 143, 626

Denissenkov, P. A. and Ivanova, N. S. and Weiss, A. 1999, A&A, 341, 181

Eddington, A. S. 1925, Observatory, 28, 73

Eddington, A. S. 1929, MNRAS, 90, 54

Endal, A. S. & Sofia, S. 1976, ApJ, 210, 184

Endal, A. S. & Sofia, S. 1978, ApJ, 220, 279

Fliegner, J., Langer, N., Venn, K. A. 1996, A&A, 308, L13

Fricke, K. 1968, ZfAp, 68, 317

Fukuda, I. 1992, PASP, 94, 271

Gies, D. R., Lambert, D. L. 1992, ApJ, 387, 318

Goldreich, P., Schubert, G. 1967, ApJ, 150, 571

Heger, A., Langer, N., & Woosley, S. E. 2000, ApJ, 528, 368

Heger, A., Woosley, S. E., Waters, R. 2000a, in *The First Stars. Proceedings of the MPA/ESO Workshop*, eds. A. Weiss, T. G. Abel, V. Hill, Springer, p. 121

Heger, A., Woosley, S. E., & Spruit, H. 2003, ApJ, in preparation

Hirschi, R., Meynet, G., Maeder. A. 2003, in Proc. IAU Symp. 215, *Stellar Rotation*, eds. A. Maeder, P. Eenens, (this volume)

Kippenhahn, R. & Thomas, H. C. 1970, in Proc. IAU Coll 4, *Stellar Rotation*, ed. A Slettebak, Reidel, Dortecht, p. 20

Kippenhahn, R., Meyer-Hofmeister, E., Thomas, H. C. 1970, A&A, 155

Kippenhahn, R. 1974, in *Late Stages of Stellar Evolution*, eds. R. J. Taylor, J. E. Hesser, IAU Symp. 66

Knobloch, E. & Spruit, H. C. 1983, A&A, 125, 59

Langer, N., Yoon, S.-C., Petrovic, J., Heger, A. 2003, in Proc. IAU Symp. 215, *Stellar Rotation*, eds. A. Maeder, P. Eenens, (this volume)

Lattimer, J. M. & Prakash, M. 2001, ApJ, 550, 426

Lindblom, L., Tohline, J. E., & Vallisneri, M. 2001, Phys. Rev. Lett, 86, 1152

MacFadyen, A., Woosley, S. E. 1999 ApJ, 524, 262

MacFadyen, A., Woosley, S. E., & Heger, A. 2001, ApJ, 550, 410

Maeder, A. 2003, A&A, 2003, in press

Maeder, A. 1997, A&A, 321, 134

Maeder, A. & Meynet, G. 1997, A&A, 321, 465

Maeder, A. & Meynet, G. 2000, ARA&A, 38, 143

Marigo, P., Chiosi, C., Kudritzki, R.-P. 2003, A&A, in press; astro-ph/0212057

Marshall, F. E., Gotthelf, E. V., Zhang, W., Middleditch, J., & Wang, Q. D. 1998, ApJ, 499, 179

Meynet, G. and Maeder, A. 2000, A&A, 361, 101

Meynet, G. and Maeder, A. 2002, A&A, 390, 561

Ostriker, J. P. & Bodenheimer, P. 1973, ApJ, 180, 171

Pinsonneault, M. H. 1997, ARA&A, 35, 557

Pinsonneault, M. H., Kawaler, S. D., Sofia, S., Demarque, P. 1989, ApJ, 338, 424

Spruit, H. C. 2002, A&A, 381, 923

Spruit, H. C. 2003, in Proc. IAU Symp. 215, *Stellar Rotation*, eds. A. Maeder, P. Eenens, (this volume)

Spruit, H. C. & Phinney, E. S. 1998, Nature, 393, 139

Talon, S., Zahn, J.-P. 1997, A&A, 317, 749

Talon, S., Zahn, J.-P., Maeder, A., Meynet, G. 1997, A&A, 322, 209

Tassoul J.-L. 2000, *Stellar Rotation*, Cambridge University Press, ISBN 0521772184

Urpin, V. A., Shalybkov, D. A., Spruit, H. C. 1996, A&A, 306, 455

Venn, K.A., Brooks, A.M., Lambert, D., Lemke, M., Langer, N., Lennon, D.J., Keenen, F.P. 2002, ApJ, 565, 571

Venn, K. A., Lambert, D. L., Lemke, M. 1996, A&A, 307, 894

Vogt, H. 1925, Astr. Nachr., 223, 229

Wasiutyński, J. 1946, Ap. Norveg., 4, 1

Woosley, S. E. 1993, ApJ, 405, 273.

Woosley, S. E., Heger, A. 2003, in Proc. IAU Symp. 215, *Stellar Rotation*, eds. A. Maeder, P. Eenens, (this volume)

Zahn, J.-P. 1974, in *Stellar instability and Evolution*, eds. P. Ledoux, A. Noels, A. W. Rogers, IAU Symp. 59, Redel, Dortrecht, p. 185

Zahn, J.-P. 1975, Mém. Soc. Roy. Sci. Liège, 6^e Serie, VIII, p. 31

Zahn, J.-P. 1992, A&A, 256, 115